PUBLICATIONS OF THE ASTRONOMICAL SOCIETY OF THE PACIFIC, 111:587–594, 1999 May

Speckle Noise and the Detection of Faint Companions

RENÉ RACINE

Observatoire du Mont Mégantic and Département de Physique, Université de Montréal, Montréal, PQ H3C 3J7, Canada; and Université Laval, Sainte-Foy, Quebec, PQ G1K 7P4, Canada; racine@astro.umontreal.ca

GORDON A. H. WALKER

Physics and Astronomy Department, University of British Columbia, Vancouver, BC V6Y 1Z4, Canada; walker@astro.ubc.ca

AND

DANIEL NADEAU, RENÉ DOYON, AND CHRISTIAN MAROIS

Observatoire du Mont Mégantic and Département de Physique, Université de Montréal, Montréal, PQ H3C 3J7, Canada; nadeaud@ere.umontreal.ca, doyon@astro.umontreal.ca, marois@astro.umontreal.ca

Received 1998 November 16; accepted 1999 February 9

ABSTRACT. Speckles dominate shot noise within the halo of adaptively corrected bright star images and, consequently, impose severe limits on ground-based attempts to directly detect planets around nearby stars. The effect is orders of magnitude greater than conventional photon noise. It depends on the dwell time of the speckle pattern, the brightness of the star, and the fraction $(1 - S)$ of residual light in the halo (S being the Strehl ratio of the image). These predictions agree well with limits found using the Canada-France-Hawaii Telescope adaptive optics bonnette. The limiting brightness for detection is proportional to $(1 - S)/S$, emphasizing the need for large Strehl ratios. Strategies to reduce speckle noise are proposed; the encouraging results of a test are presented.

1. INTRODUCTION

The direct imaging of faint companions close to nearby stars, in the search for brown dwarfs or giant planets, is a difficult but important observational challenge. Precision radial velocity (PRV) (Mayor & Queloz 1995; Marcy & Butler 1996) and astrometric results (Gatewood 1996), following long-term PRV studies (Walker et al. 1995), have uncovered with varying degrees of confidence a number of very low mass companions, enhancing hopes that such objects may be detectable around nearby stars by high-performance direct-imaging techniques. Image data, combined with radial velocity results, would allow a complete determination of the system geometry and dynamics.

A number of authors have discussed the challenge posed by the detection of companions against the glare of a primary brighter by many orders of magnitude at separations of 1″ or less. Near-infrared speckle interferometry by Henry & McCarthy (1990) has set limits of Δm_H(companion − primary) ~ 4 mag at separations of ~1″ for a primary of $m_H \sim 7$. Coronagraphic techniques have been discussed by Nakajima (1994) and by Ftaclas (1994). Nakajima estimates that coronagraphic imaging with a low-order adaptive optics (AO) system on a 6.5 m telescope could detect Jupiter-size planets about a solar-type star ($\Delta m_H \sim 20$) at $\rho \sim 1\farcs5$ with a signal-to-noise ratio (S/N) of 3 in 10^4 s. His calculations are based on the optimistic assumption that the noise of the primary-image residual halo arises from the statistics of independent photons. The significance of correlated speckle noise has been commented on by many authors (Angel 1994, 1995; Langlois et al. 1998; Olivier, Gavel, & Brase 1995; Roddier 1995; Roddier & Roddier 1995; Ryan et al. 1998; Stadhl & Sandler 1995). Since each speckle can contain a very large number F_s of detected coherent photons, the background noise density is then given by $\sqrt{n_s F_s}$, where n_s is the number of speckles per unit area, rather than by $\sqrt{n_s F_s}$, as would be the case for independent photons. The situation is analogous to that of surface brightness fluctuations over the unresolved bulges of galaxies (Tonry & Schneider 1988) where the statistics are controlled by the number of *stars* rather than by the number of photons.

Angel argues that, for a wave front compensated in phase and intensity by a very high order AO system, the speckle patterns will be uncorrelated between each correction cycle. This would be so because photon noise over the hundreds of thousands of AO channels would randomize the phase errors after each correction. In Angel's scenario, the compensated Strehl ratio (S) is very close to unity and the closed loop AO bandwidth is very high (2–3 kHz). Consequently, the residual halo contains a small fraction $(1 - S)$ of the primary flux. Furthermore, F_s is much reduced as the speckle lifetime is limited, by hypothesis, to the correction

time that randomizes residual phase errors rather than to the longer natural speckle dwell time. This, and the fact that nearly all of the companion's flux would be contained in the diffraction limited core of its point-spread function (PSF), would allow us to reach a spectacular $\Delta m \sim 20$ at shorter wavelengths (smaller PSF area, fainter speckles) with an 8 m class telescope in an integration time of ~ 1 hr.

In this paper, we explore the consequences of speckle noise for the detection of faint companions when more modest AO systems, such as the Canada-France-Hawaii Telescope (CFHT) AO "bonnette" (AOB), are used. Section 2 develops general ideas and equations. They are applied in § 3 to yield detection predictions based the CFHT AOB known performances (Rigaut et al. 1998). It will be seen that speckle noise is, by very far, the dominant noise component with bright primaries, an expectation confirmed by the analysis of actual images. Section 4 concludes by outlining strategies capable of removing much of the speckle noise from the data. The encouraging results obtained with one of them are presented.

2. BASIC IDEAS AND EQUATIONS

In this section, we wish to explicitly derive the S/N of the companion image against the background noise. To do this, we need models for the PSF and for the underlying noise components.

2.1. PSF Model

The AO-compensated long-exposure PSF of the primary star is modeled as the sum of a diffraction-limited core and a residual halo. The total detected flux F_* (number of photoevents or electrons) in this PSF is

$$F_* = \frac{\pi}{4} D^2 q f_0 \, 10^{-0.4 m_*} t \, , \tag{1}$$

where D is the diameter of the telescope aperture (in meters), q is the global quantum efficiency, f_0 is the flux density from a zero-magnitude star in the bandpass (in photons m^{-2} s^{-1}), m_* is the stellar magnitude, and t is the integration time (in seconds).

The intensity profile of the image core, $I_{\rm core}(\theta)$, is that of the diffraction pattern of the telescope and contains a fraction S of the total number of detected photoevents F_*:

$$I_{\rm core}(\theta) = S F_* \, f_{\rm core}(\theta) \, . \tag{2a}$$

The adopted profile for the residual halo, $I_{\rm halo}(\theta)$, is a fit to the long-exposure AO-compensated PSF produced by the CFHT AOB after subtraction of the image core. $I_{\rm halo}(\theta)$ contains a fraction $(1 - S)$ of F_*:

$$I_{\rm halo}(\theta) = (1 - S) F_* \, f_{\rm halo}(\theta) \, . \tag{2b}$$

A convenient Moffat (1969) profile of index $\beta = 11/6$ and unit volume is used for the numerical calculation of the shape function $f_{\rm halo}(\theta)$. It is characterized by an FWHM intensity $W_{\rm halo}$, which contains $\sim 25\%$ of its flux, and a $\theta^{-11/3}$ decay beyond a few $W_{\rm halo}$, as appropriate to a turbulence-degraded profile (Roddier 1981):

$$f_{\rm halo}(\theta) = \frac{0.488}{W_{\rm halo}^2} \left[1 + \frac{11}{6} \left(\frac{\theta}{W_{\rm halo}} \right)^2 \right]^{-11/6} \, . \tag{3}$$

The PSF of the companion is assumed to contain a fraction S of its flux F_c within a "PSF area" corresponding to the solid angle $\pi(\lambda/D)^2$ where its net signal is to be detected against noise. This definition of the PSF area recognizes that, in practice, it is the sharp core of the companion image that will enable its detection, its broader halo still being swamped by background noise. In what follows, numerical values of θ and λ/D are expressed in arcseconds, e.g., $0.2063\lambda[\mu\text{m}]/D[\text{m}]$.

2.2. Background Signals and Noises

We now consider the various sources of background light recorded within a PSF area. For the ith source, the total number of statistically independent events (not necessarily photoevents) detected per unit area is n_i and their mean brightness, measured in photoevent units or electron counts, is B_i. Thus the signal from this ith source in the PSF area is $\pi(\lambda/D)^2 n_i B_i$, and its dispersion, which contributes to local Poisson noise, is $\sqrt{\pi}(\lambda/D)\sqrt{n_i} B_i$. For independent photoevents, $B_i \equiv 1$ and the variance of their noise is their signal.

2.2.1. Photon, Read, and Sky Noises

The noise under the PSF of the companion is then composed of the following terms:

1. The photon noise of the coherent core of the primary, whose variance is

$$\text{var(core photons)} = \pi(\lambda/D)^2 I_{\rm core}(\theta) \, . \tag{4a}$$

2. The photon noise of the incoherent halo of the primary, whose variance is

$$\text{var(halo photons)} = \pi(\lambda/D)^2 I_{\rm halo}(\theta) \, . \tag{4b}$$

3. The read noise σ_r (in electrons per pixel per read), whose variance for the $t/\Delta t$ ($\Delta t =$ read interval) reads of an

observation sequence with a detector scale s (pixel arcsec^{-1}) is

$$\text{var(read noise)} = \pi(\lambda/D)^2\sigma_r^2(t/\Delta t)s^2 \ . \quad (4c)$$

4. The sky noise, whose variance is

$$\text{var(sky noise)} = \pi(\lambda/D)^2 F_{\text{sky}} = \pi(\lambda/D)^2(\pi/4)D^2 q f_0\, 10^{-0.4 m_{\text{sky}}} t \ , \quad (4d)$$

where m_{sky} is the sky brightness in mag arcsec^{-2}.

5. Finally, we come to the speckle noise. To understand how this can be estimated, it may be useful to give a brief, qualitative explanation of the speckle formation process and of speckle statistics. A more rigorous analysis can be found in Roddier's (1981) review.

2.2.2. *Speckle Formation and Statistics*

The *uncompensated* short-exposure image of a point source formed by a corrugated wave front is composed of numerous short-lived speckles. These result from the interference of light from many coherent patches, of typical diameter r_0, distributed over the full aperture of the telescope. A single r_0-size subpupil would form a PSF of width $\sim\lambda/r_0$ imposed by diffraction. Two such subpupils, separated by a distance $\sim D$, constitute a two-beam interferometer: the intensity of the PSF they jointly produce is now modulated by a pattern of linear interference (Young) fringes, normal to the line joining the subapertures, and of width $\sim\lambda/D$. As a result of the randomly varying phase difference (relative tilt) between the two subapertures, this fringe pattern moves within the broad PSF envelope. The introduction of a third subaperture, noncollinear with the first two, gives three nonredundant pairs of subapertures and result in the appearance of three intersecting patterns of moving fringes. Where these fringes interfere constructively, an enhanced bright "speckle" of width $\sim\lambda/D$ appears. Filling the pupil with r_0-size subpupils synthesizes a filled-aperture interferometer affected by random phase errors and produces the full speckle pattern. There is room for $k(D/r_0)^2$ adjacent speckles of size $\sim\lambda/D$ within the "seeing" disk of width $\sim\lambda/r_0$, an analysis of the wave front statistics being required to estimate the value of the filling factor k with some precision. Roddier (1981) and Roddier et al. (1982) show that when $D/r_0 \gg 1$ or $S_{\text{natural}} \ll 1$,

$$k = 0.342 \ . \quad (5)$$

The speckle lifetime τ_0 is

$$\tau_0 \sim r_0/\Delta v \ , \quad (6)$$

where Δv is the velocity dispersion in the turbulent seeing layers across the telescope line of sight. Each speckle covers an area $\sim\pi(\lambda/D)^2/k$; their number per unit area is

$$n_s \simeq \frac{0.342}{\pi(\lambda/D)^2} \ . \quad (7)$$

In an AO-compensated image, a fraction S of the flux F_* is transferred into a bright central speckle, leaving $(1-S)F_*$ into halo speckles that, by time averaging, produce the smooth, long-exposure halo. The central core arises because relative tilt errors approaching zero, hence constructive interference at the PSF center, are more likely in a compensated wave front. In terms of the wave front phase structure function, the central core is explained by the increased coherence that compensation produces: low-order aberrations are removed, and the structure function saturates at large separations. Compensation also leads to an enlargement of the coherent areas in the pupil, hence an effective increase in r_0: a shrinkage of the halo size results. For the CFHT AOB operating with a bright reference star, which is the case of interest here, W_{halo} is reduced, and r_0 is increased, by a factor of ~ 1.5 (Rigaut et al. 1998).

2.2.3. *Speckle Noise and Signal-to-Noise Ratio*

The variability of the wave front corrugation results in "speckle boiling" and is the source of speckle noise. The structure of the speckle pattern changes randomly over a small fraction of a second and a given area of the detector will sample a different pattern after each τ_0 interval. But the speckle noise variance is *not* simply equal to the number of speckles recorded in this area times the mean speckle brightness. This is so because speckles are *not* independent events, by the nature of the interference that produces them, and their number per unit area in the image is necessarily constant (eq. [7]). Speckle noise arises from *registration variations* between the evolving speckle pattern in the focal plane and the boundary of a given PSF area in that plane; in other words, as the speckle pattern evolves, speckles grow and fade across the fixed boundary of the PSF area and the total flux in this area fluctuates. Numerical simulations were carried out to assess this noise level. Fluxes were computed through circular apertures of diameters $2(\lambda/D) \le \Delta \le 10(\lambda/D)$, randomly located on a $D/r_0 \gg 1$ speckle pattern. Both computer-generated and actual speckle patterns were used. The results agreed with a simplistic analytical estimate, namely, that the integral of a two-dimensional positive harmonic function over a randomly located area of any size yields fluctuations about the mean which average $\frac{1}{4}$ of the integral over 1 cycle, or $\frac{1}{4}$ of the flux F_s in a single speckle in our case. Thus, after t/τ_0 speckle pattern realizations, the speckle variance in the PSF (or any) area will be

$$\text{var(speckles)} \simeq \frac{F_s^2}{16}\frac{t}{\tau_0} \ . \quad (8)$$

This assumes $t > \tau_0$ such that the exposure records the signal from a speckle over its full lifetime. The possibility of "defeating" speckle noise by co-adding separate exposures for which $t \ll \tau_0$ will be mentioned in § 4. The speckle brightness F_s varies radially in the image, inner speckles being brighter, a consequence of the intensity profile of the diffraction pattern of a single r_0-size subpupil from which the speckle pattern is "carved." At a given radius θ in the PSF halo, $F_s(\theta)$ is the ratio between the halo surface brightness recorded in a speckle lifetime and the number of speckles per unit area (eq. [7]):

$$F_s(\theta) \simeq \frac{\pi(\lambda/D)^2}{0.342} I_{\rm halo}(\theta) \frac{\tau_0}{t} . \quad (9)$$

This assumes that at all times the radial profile of speckle brightness follows a same centrosymmetric $f_{\rm halo}(\theta)$ relation. In practice, this is not the case, especially for natural images, because atmospheric seeing continuously distorts the image shape. Consequently, the brightness of speckles at a given θ will vary with time. This, however, does not affect the estimate of speckle noise, which would be unchanged if the concept of mean speckle brightness $\langle F_s \rangle$ were used.

Figure 1 shows natural and AO-compensated short-exposure images of a star obtained at the CFHT. The structure of the speckle pattern and the increase in speckle brightness at smaller offsets are clearly seen. From equations (2a), (2b), (8), and (9), one obtains

$$\text{var(halo speckles)} \simeq 1.7\pi[(\lambda/D)^2(1 - S)F_* f_{\rm halo}(\theta)]^2 \frac{\tau_0}{t} . \quad (10)$$

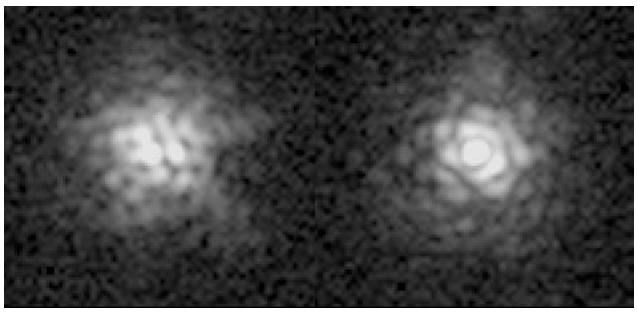

FIG. 1.—Short-exposure (0.1 s) natural (*left*) and AO-compensated (*right*) images of a star obtained with the CFHT AOB at $\lambda = 1.6$ μm and $D/r_0 \sim 4$. The gray scale is logarithmic in intensity, and the read noise is apparent in the background. Note the increasing speckle brightness toward the PSF center and the appearance of the bright central core in the compensated image.

The ratio of the companion signal SF_c to the halo speckle noise in the PSF area is the S/N(halo speckles) imposed by halo speckles to the detection of the companion:

$$\text{S/N(halo speckles)} \equiv \frac{SF_c}{\sqrt{\text{var(halo speckles)}}} . \quad (11a)$$

Substituting equation (10) in equation (11a) and combining the numerical constants yields

$$\text{S/N(halo speckles)} \simeq 0.43\left(\frac{D}{\lambda}\right)^2 \frac{S}{1 - S} \frac{F_c}{F_*} \frac{1}{f_{\rm halo}(\theta)} \left(\frac{t}{\tau_0}\right)^{1/2} , \quad (11b)$$

where the compensated value of r_0 is used when appropriate to estimate τ_0. Note that the S/N increases dramatically as $S \to 1$. It is independent of qf_0, and the achievable brightness ratio between companion and primary is independent of F_*. In the speckle-limited regime, each speckle contains a large number of photoevents; changing q or f_0 changes that number but also the number of photoevents in F_c and leaves S/N(halo speckles) the same. It is also seen that large-aperture telescopes working at short wavelengths are, in principle, much preferable for the detection of faint companions *if* the Strehl ratio of the compensated image can be maintained at large D/r_0. This will be a challenging task with the high-order AO systems this requires. With equation (3) and $W_{\rm halo} \approx \lambda/r_0$, equation (11b) becomes

$$\text{S/N(halo speckles)} \simeq 1.2 \frac{S}{1 - S}\left(\frac{D}{r_0}\right)^2 \frac{F_c}{F_*} \times \left[1 + \frac{11}{6}\left(\frac{\theta}{\lambda/r_0}\right)^2\right]^{11/6}\left(\frac{t}{\tau_0}\right)^{1/2} , \quad (11c)$$

and

$$S \simeq \exp\,[-0.3(D/r_0)^{5/3}N^{-5/6}] . \quad (12)$$

We evaluate the value of D/r_0 that maximizes the product $S(1 - S)(D/r_0)^2$ in equation (11c); that value is

$$(D/r_0) \simeq 1.2\sqrt{N} . \quad (13)$$

In practice, the value of N in equation (13) should be the *effective* number of actuators N_e, that which a system of unit efficiency requires to achieve the same Strehl ratio as an actual system on bright stars. High-performance AO systems such as the CFHT AOB have efficiencies $N_e/N \sim 0.5$ (Rigaut et al. 1998; Roddier 1998). For the CFHT AOB ($N = 19$), $N_e \simeq 9$ and $(D/r_0)_{\rm optimal} \simeq 3.5$: optimal performance with the 3.6 m CFHT occurs when $r_0 \simeq 1.0$ m or at $\lambda \simeq 2.0$ μm by typical 0".4 seeing at that wavelength.

Because speckle noise is dominant at small offsets (see below), our ongoing search for faint companion images close to bright primaries is being done in the H band ($\lambda \simeq 1.6$ μm). Finally, including the various noise components discussed above, the square of the signal-to-noise ratio of the faint companion image in the PSF area is

$$(\mathrm{S/N})^2 \simeq (S^2 F_c^2)/\mathrm{var}(\text{halo speckle} + \text{halo photons} + \text{core photons} + \text{read noise} + \text{sky noise}) , \quad (14)$$

which leads to the following explicit expression for the detectable brightness ratio between companion and primary:

$$\frac{F_c}{F_*} \simeq \sqrt{\pi}\left(\frac{\lambda}{D}\right)\frac{\mathrm{S/N}}{S} \times \left\{1.7\left[\frac{\lambda}{D}(1-S) f_{\mathrm{halo}}(\theta)\right]^2 \frac{\tau_0}{t} \quad \text{(speckles)} + (1-S)\frac{f_{\mathrm{halo}}(\theta)}{F_*} \quad \text{(halo photons)} + S\frac{f_{\mathrm{core}}(\theta)}{F_*} \quad \text{(core photons)} + \sigma_r^2 \frac{t}{\Delta t}\frac{(\text{pixels arcsec}^{-1})^2}{F_*^2} \quad \text{(read noise)} + \frac{F_{\mathrm{sky}}}{F_*^2} \quad \text{(sky noise)}\right\}^{1/2} . \quad (15)$$

Recall that numerical values of angles in equation (15), such as θ and (λ/D), are to be converted to arcseconds to be consistent with the traditional units adopted for detector scale (pixels arcsec^{-1}) and sky brightness (mag arcsec^{-2}).

3. CALCULATIONS AND OBSERVATIONS

The five terms in the curly brackets of equation (15) are all related by a same factor to the variances of the noise components. Thus the ratio of speckle noise to photon noise in the halo is

$$\frac{\mathrm{var(speckles)}}{\mathrm{var(halo\ photons)}} \simeq 1.7(1-S)\left(\frac{\lambda}{D}\right)^2 \frac{r_0}{t\Delta v} F_* f_{\mathrm{halo}}(\theta) , \quad (16a)$$

which, by equations (1) and (3) and with $W_{\mathrm{halo}} \simeq (\lambda/r_0)$, becomes

$$\frac{\mathrm{var(speckles)}}{\mathrm{var(halo\ photons)}} \simeq 0.5(1-S)\frac{r_0^3}{\Delta v} q f_0 \times \frac{10^{-0.4 m_*}}{[1 + \frac{11}{6}(\theta/W_{\mathrm{halo}})^2]^{11/6}} . \quad (16b)$$

For typical values of the parameters ($S = 0.5$, $q = 0.2$, and $r_0 = 1$ m at 2 μm or $W_{\mathrm{halo}} = 0\farcs4$, $\Delta v = 10$ ms^{-1}, and $f_0 = 3 \times 10^9$ photons m^{-2} s^{-1} for the H band), the leading terms in equation (16b) amount to $\sim 2.5 \times 10^6$ and the ratio is larger than unity at $\theta < W$ for $m_* < 16$. It follows that speckle noise vastly dominates shot noise in the halo of bright stars. This is the main point of this paper.

Figure 2 illustrates the results of variance calculations for an $m_H = 8$ primary and typical CFHT AOB performances in the H band with the NICMOS-based Montreal Infrared Camera (MONICA) (Nadeau et al. 1994) in its high-resolution (30 pixels arcsec^{-1}) mode. Speckle variance dominates by a factor of $\sim 10^4$! This reduces the Δm for which a companion can be detected by ~ 5 mag compared with what would be achieved against the statistics of independent photons. This Δm shortfall depends on the brightness of the primary; it would be ~ 7.5 mag at $m_H = 3$ and would become negligible only for primaries so faint ($m_H > 17$) that the sky and read noise would dominate the detection of their companions.

The results of these calculations were compared to actual noise statistics measured on MONICA images ($\sigma_r \sim 25e^-$) obtained during the full Moon [$m_H(\mathrm{sky}) \sim 15$] with the

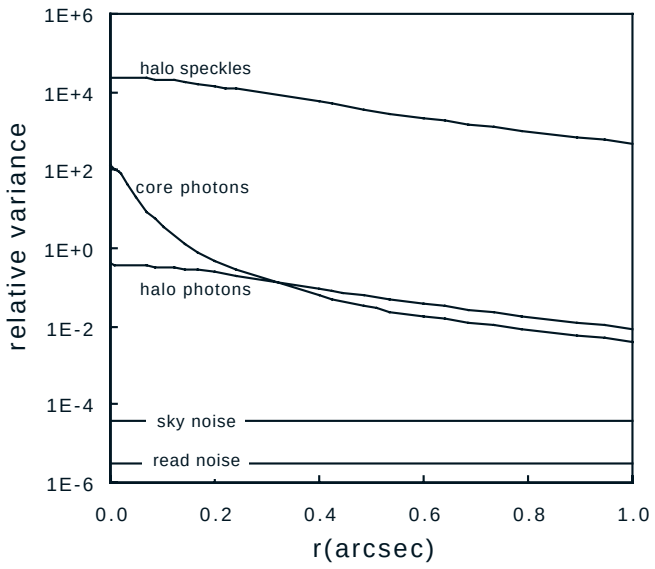

FIG. 2.—Relative importance of the variances for the different noise components. The models parameters are $qf_0 = 6 \times 10^8$, $D = 3.6$ m, $\lambda = 1.6$ μm, $S = 0.5$, $m_* = 8$, $m_{\mathrm{sky}} = 16$, $s = 30$ pixels arcsec^{-1}, $\sigma_r = 30$ electrons, $t = 200$ s, $r_0 = 1$ m, and $\tau_0 = 0.1$ s.

CFHT AOB in 1996 November. The seeing was poor ($\sim 1''.1$ FWHM), the speckle pattern quite extended, and only a meager Strehl of ~ 0.15 could be achieved. A value of $\tau_0 \sim 0.04$ s was estimated from the surface brightness fluctuations in 0.1 s exposure PSF images. The central $0''.6$ diameter area of the PSF was attenuated by a tapered coronagraphic mask that prevented detector saturation. Twenty consecutive H-band frames of the $m_H = 4.4$ star 55 Cnc, each one being the co-addition of 30 1.2 s exposures, were used to form 10 difference images between adjacent pairs. These were co-added and the composite convolved with a Gaussian filter of FWHM $= \lambda/D$ (3 pixels). A median-filtered image of itself was subtracted from the composite to reduce low-frequency fluctuations caused by centering differences between individual images. The noise amplitude (1 σ) in the resulting image was then measured in annuli of increasing radii about the PSF center. Figure 3 shows this noise amplitude, expressed as a magnitude difference with respect to the unattenuated PSF peak intensity, as a function of radius. The line represents equation (15) for the parameter values given above for the observations; it is *not* a fit to the data but follows them fairly well. A model free of speckle noise would lie 3.3 mag above the one shown at $\theta = 1''$. Within the central mask area, the data fall above the (unfiltered) model because the amplitude of the observed fluctuations are attenuated. The general agreement between data and model is a convincing experimental demonstration that speckle noise is indeed the major hurdle with which ground-based detection of faint close companions to bright stars must contend.

4. DEFEATING SPECKLE NOISE?

Faced with the speckle noise "tax," one could try to imagine various ways of escaping it. The returns would be rich indeed, as shown by Figure 4. For instance, a Sun-Jupiter system ($\Delta m \simeq 20$) would easily be detectable with an 8 m class telescope at a distance of 10 pc ($m_* \simeq 4$, separation $\simeq 0''.5$).

Co-adding very short exposures, separated by a delay longer than the speckle lifetime, or using very narrowband or strongly absorbing filters, such that each speckle contains fewer than 1 detected photon, could defeat speckle noise. But since the delay between consecutive exposures would need to be at least t_0, it is easily shown from equation (11c) that the S/N for companion detection per unit telescope time cannot be greater than in the speckle regime, even assuming zero read noise.

A more efficient approach would be to very much increase the number and spatial spread of *halo* speckles and to make their lifetime very short: they would then be very much fainter and the halo would be "washed out." This would require artificially making the correlation length r_0 of the compensated wave front very small while preserving the saturation of the phase structure function at large separations, to maintain the partial coherence over the pupil that gives rise to the image core. It may be possible to achieve that goal with a randomly time variable, high spatial frequency, low-amplitude phase or "scatter" plate inserted at a pupil image, after the wave front sensor to preserve its performance. The price to pay would be a multiplication of the Strehl ratio S, by a factor $\sim S$, because

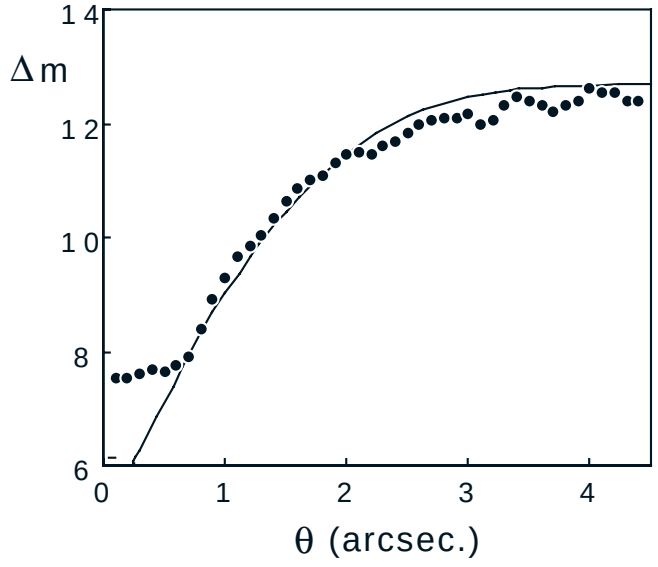

FIG. 3.—Observed (*dots*) and calculated (*line*) 1 σ detection limits as functions of the companion separation. The speckle-limited model is *not* a fit to the data. See text for discussion.

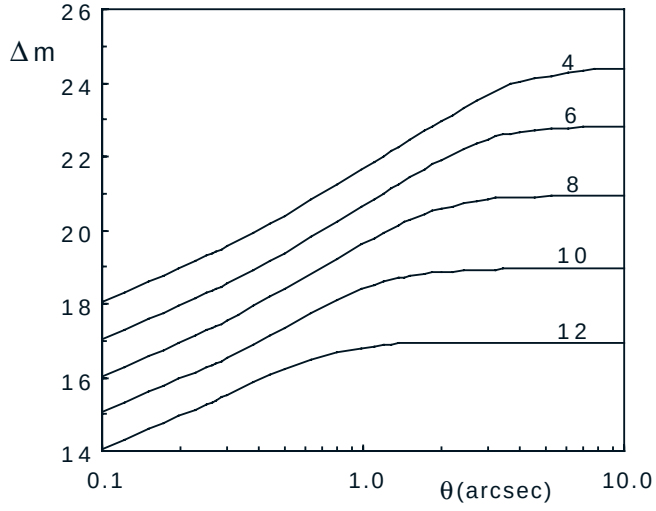

FIG. 4.—Calculated 3 σ detection thresholds as a function of m_* for an 8 m telescope freed of speckle noise at $S = 0.7$ in the H band; 10,000 s integration.

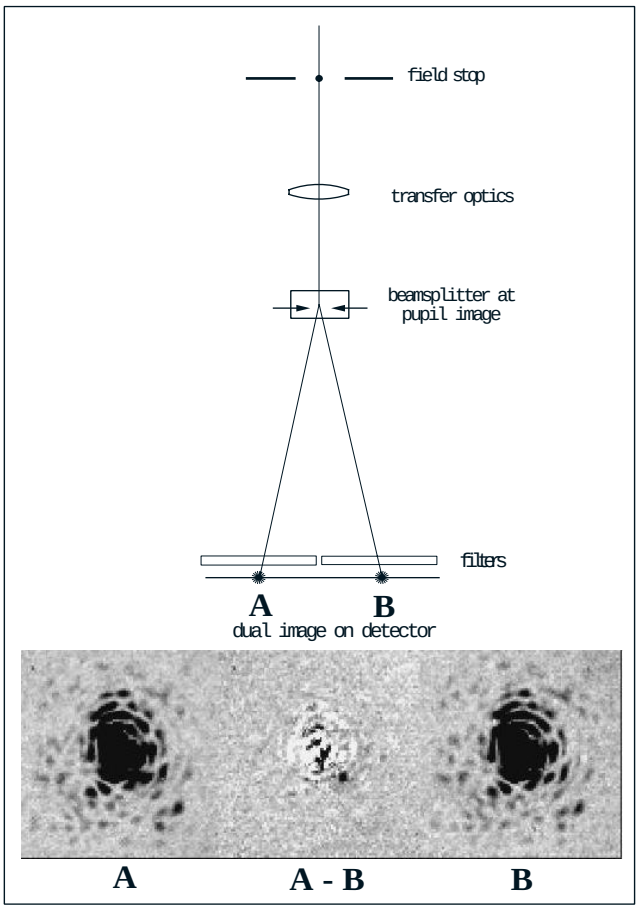

FIG. 5.—Dual-imaging arrangement, resulting images, and their difference. The three displays have the same stretch. The technique is seen to be effective at subtracting the speckle pattern. The artificial image of a companion, 5 mag fainter that its primary and 0.″5 away, has been inserted in the image on the left. It is clearly visible in the difference image.

$S \sim \exp(-\sigma_\phi^2)$ and the phase variance σ_ϕ^2 over large separations would be nearly doubled. The benefit could still be substantial when S is large.

Space observations, such as with the *Hubble Space Telescope*, benefit from high Strehl ratios and relatively stable instrumental speckle patterns that could be removed by subtracting images of different stars, as can be done for the fixed speckles of ground-based telescopes. Whether space telescopes will prove superior to large ground-based telescopes will depend on the relative values of the S/N(speckles) for these facilities. PSF stability and ability to accurately flat-field the data will also be crucial.

An obvious but still unavailable solution at ground-based telescopes is to strive for $S \rightarrow 1$ at short wavelengths, where r_0 and t_0 are small, hence the speckles fainter and more quickly averaged, especially if their lifetime is limited by the very short response time of the AO system. This is the Angel (1994, 1995) scenario.

To approach the photon-noise limit with more modest AO systems, one must devise an observing strategy that enables the *subtraction* of the speckle pattern. This can be done with pairs of images taken simultaneously (identical speckle patterns) in two narrowband filters closely adjacent in wavelength (the speckle pattern is chromatic) through which the contrast between primary and companion is very different, such as across the methane band head at 1.59 μm in cool brown dwarfs (Rosenthal, Gurwell, & Ho 1996). The limiting factor then becomes the flat-fielding noise at spatial frequencies of $\sim D/\lambda$. To reduce the speckle noise below photon noise around bright stars, the subtraction, hence the flat-fielding, has to be accurate to $\sim 10^{-3}$ (see Fig. 2), a goal that should be possible to reach (Tyson 1986; Kuhn & Loranz 1991).

A first experiment with this technique was carried out at the end of a CFHT observing run, in 1997 February. A beam splitter was inserted at a pupil in the MONICA cryostat, and pairs of images of an aberrated artificial star ($S \sim 0.7$) were recorded through a CO (2.30/0.03 μm) and then through a K-continuum (2.26/0.05 μm) filter. The setup did not allow filtering each image of the pair by different filters, hence the use of the artificial star whose aberrations are constant. Figure 5 illustrates the setup and shows two images, each taken in different filters and from alternate sides of the NICMOS array, and the difference image obtained after appropriate intensity and dimensional scaling to compensate for differences in throughput and effective wavelengths. The subtraction reduces the intensities in the speckle pattern by a factor of ~ 50. As an

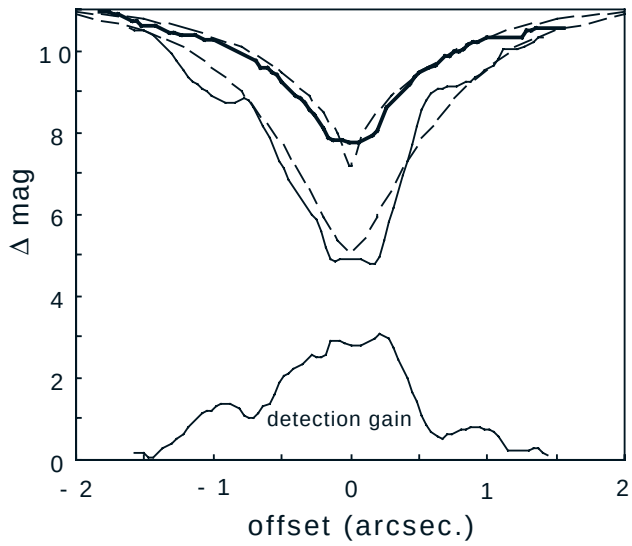

FIG. 6.—Measured 3 σ detection thresholds, given as magnitude differences (companion − primary) in a raw (*thin line*) and a "despeckled" (*thick line*) PSF. The detection gain (*bottom curve*) is the difference between the two. CFHT AO system, 400 s exposure, $m_H = 7$. Dashed lines are model calculations.

amusing exercise, an artificial companion, 5 mag fainter than the primary, was added to one of the original images at a separation of 0".5. It is clearly visible in the difference image of Figure 5.

A more quantitative and realistic measure of the gain realized in practice was later made using long exposures taken on a real star during a subsequent CFHT run (1997 December), when simultaneous dual imaging was possible. First, a heavily smoothed version of one of the dual PSF images was subtracted from itself, and the rms noise level in the difference image was measured in annuli of increasing radii. The ratio of this noise level to the peak intensity of the original PSF measures the detection threshold as a function of radius in the conventional, single-frame observing mode. Then, one of the two simultaneous images was subtracted from the other and the rms noise in the difference image was measured, thereby yielding the detection threshold in the dual-frame observing method. The results of this exercise are shown in Figure 6. It is seen that "speckle subtraction" has achieved a detection gain of nearly 3 mag at small offsets, in good agreement with models calculated with the precepts of § 2 and which use actual values of the observational parameters as inputs. This demonstrates, again, that speckle noise is the dominant factor at smaller offsets and that the dual image technique is effective at reducing it.

We are indebted to Malcolm Northcott, François Rigaut, Francois Roddier, and Farrok Vakili for enlightening discussions of speckle statistics and to CFHT's Derrick Salmon and Jon Serveld for help with the production of the coronagraphic masks. The necessary modifications to MONICA were designed by Philippe Vallée and carried out by Jean-Eudes Samuel in the UdeM machine shop. The image processing skills of Jean-Pierre Véran were extensively relied upon to extract the above results. Guest investigator privileges at the Canada-France-Hawaii Telescope are gratefully acknowledged. This work was supported in part through grants from the Natural Sciences and Engineering Research Council, Canada, and from Fonds FCAR, Québec.

REFERENCES

Angel, J. R. P. 1994, Nature, 368, 203
———. 1995, Ap&SS, 223, 117
Ftaclas, C. 1994, in 15th NSO/Sacramento Peak Workshop, IR Tools for Solar Astrophysics: What's Next?, ed. J. R. Kuhn & M. J. Penn (Singapore: World Scientific), 181
Gatewood, G. 1996, BAAS, 28, 885
Henry, T. J., & McCarthy, D. W. 1990, ApJ, 350, 334
Kuhn, J. R., & Loranz, D. 1991, PASP, 103, 1097
Langlois, M., Sandler, D., Ryan, P., & McCarthy, D. 1998, Proc. SPIE, 3353, 189
Marcy, G., & Butler, P. 1996, ApJ, 464, L147
Mayor, M., & Queloz, D. 1995, Nature, 378, 355
Moffat, A. F. J. 1969, A&A, 3, 455
Nadeau, D., Murphy, D. C., Doyon, R., & Rowlands, N. 1994, PASP, 106, 909
Nakajima, T. 1994, ApJ, 425, 348
Olivier, S. S., Gavel, D. T., & Brase, J. M. 1995, Ap&SS, 223 181
Rigaut, F., et al. 1998, PASP, 110, 52
Roddier, F. 1981, Prog. Opt., 19, 281
———. 1995, Ap&SS, 223, 109
———. 1998, PASP, 110, 837
Roddier, F., Gilli, J. M., & Lund, G. 1982, J. Opt. (Paris), 13, 263
Roddier, C., & Roddier, F. 1995, Ap&SS, 223, 183
Rosenthal, E. D., Gurwell, M. A., & Ho, P. T. P. 1996, Nature, 384, 243
Ryan, P. T., Fugate, R. Q., Langlois, M., & Sandler, D. G. 1998, Proc. SPIE, 3353, 107
Stadhl, S., & Sandler, D. G. 1995, ApJ, 454, L153
Tonry, J., & Schneider, D. P. 1988, AJ, 96, 807
Tyson, J. A. 1986, J. Opt. Soc. Am., A3, 2131
Walker, G. A. H., Walker, A. R., Irwin, A. W., Larson, A. M., Yang, S. L. S., & Richardson, D. C. 1995, Icarus, 116, 359